

See discussions, stats, and author profiles for this publication at: <https://www.researchgate.net/publication/273481258>

Self-sensing properties of smart composite based on embedded buckypaper layer

Article in *Structural Health Monitoring* · February 2015

DOI: 10.1177/1475921714568405

CITATIONS

4

READS

32

4 authors, including:



Leng Jinsong

Harbin Institute of Technology

381 PUBLICATIONS 4,215 CITATIONS

SEE PROFILE

Some of the authors of this publication are also working on these related projects:



Electroactive polymers [View project](#)



Structural health monitoring [View project](#)

All content following this page was uploaded by [Leng Jinsong](#) on 10 March 2016.

The user has requested enhancement of the downloaded file. All in-text references [underlined in blue](#) are added to the original document and are linked to publications on ResearchGate, letting you access and read them immediately.

Self-sensing properties of smart composite based on embedded buckypaper layer

Zhichun Zhang¹, Hanqing Wei¹, Yanju Liu² and Jinsong Leng¹

Abstract

Advanced polymer matrix composite is a brittle material, and local fibre, matrix fracture and bonding delamination will cause the catastrophic failure of the composite. So, the strain and damage structural health monitoring of the composite material and its structures is very important for its applications. Based on the piezo-resistivity effect, micro-pore structure and resin infiltration properties of buckypaper, in this study, we develop a self-sensing composite based on embedded buckypaper, which only acts as a sensing layer to monitor the strain and damage of the composite. The strain and damage of the composite are reflected by the resistance change in the embedded buckypaper. The strain sensing properties of the buckypaper/epoxy film with different buckypaper aspect ratios 3:1, 6:1, 9:1, 12:1 and 15:1 were studied with voltammetry method, and the results indicated that there were two-stage relation between resistance change and strain, and under low strain level ($\sim 2000 \mu\epsilon$), the strain sensitivity was nonlinear and unstable, but in the high strain level, the strain sensitivity was high with strain factor about 6.2, which was independent of the dimension of buckypaper layer. The self-sensing composite made of glass fibre-reinforced composite with embedded buckypaper shows the same strain sensing properties as buckypaper/epoxy film; at same time the damage revolution of the composite could be monitored by resistance development. The scanning electron microscope characterization demonstrated that the resin can penetrate into buckypaper of the composite and form strong bonding interface. The self-sensing composite can be applied in further large-scale advanced polymer composite materials and structures structural health monitoring (strain monitoring and damage detecting).

Keywords

Buckypaper, piezo-resistive effect, strain sensing, structural health monitoring

Introduction

Advanced polymer matrix composite, for its light weight, high strength and corrosion resistance, is widely applied in aeronautical, aerospace, automobile and civil engineering and wind turbine blade structures. The composite structures are often subjected to high stress, fatigue and impact loads, which cause the local fibre breaking, matrix cracking or bonding interface delamination, and then will lead to the sudden failure of the composite. Up to now, monitoring the strains and damages is the main problem of composite material structural health monitoring. In the last two decades, several monitoring methods for composite structural health monitoring emerged, such as the strain monitoring based on fibre Bragg grating (FBG), passive damage monitoring according to acoustic emission principle using lead zirconate titanate (PZT) transducer and

active damage monitoring and location based on Lamb wave using at least two PZT transducers (one for actuation and other for sensing).^{1–4} In the above three monitoring methods, the size of the sensors (FBG, PZT) is relatively large comparing to the fibre of the composite, and sensor embedment will lead to a decrease in mechanical properties of the composite.

¹Center for Composite Materials and Structures, Harbin Institute of Technology (HIT) Science Park, Harbin, P.R. China

²Department of Aerospace Science and Mechanics, Harbin Institute of Technology (HIT), Harbin, P.R. China

Corresponding author:

Jinsong Leng, Center for Composite Materials and Structures, Harbin Institute of Technology (HIT) Science Park, No. 2 YiKuang Street, Harbin 150080, P.R. China.

Email: lengjs@hit.edu.cn

Because of the excellent mechanical property and nano size effect of carbon nanotube (CNT), CNT can be used as the filler of advanced polymer matrix composites and polymers to enhance their mechanical performance, such as improving the bonding interface,⁵ increasing composite surface wearability⁶ and improving polymer heating resistance. Most importantly, CNT can serve as conducting filler of composites or polymers to improve their conductivities, which act as antistatic, electromagnetic interference (EMI) shielding and electric heating materials. Moreover, in CNT-filled polymers or composites, there is reversible correlation between the mechanical force of deformation and their electric resistance, which is called the piezo-resistive effect. In the literature,^{7–9} the CNTs (single-walled carbon nanotube (SWCNT) and multi-walled carbon nanotube (MWCNT)), polymer matrix (thermosetting, thermoplastic), CNT load (0.05–10 wt%) and the other effecting factors were considered. The conductivity and gauge factor of the sensors increased with the increase in CNT load. But under high the CNTs filling percentage, there is a nonlinear sensing relationship between the resistance change and strain. This is caused by the non-uniform CNT distribution in the sensors at high CNT load. For the large specific surface area of CNTs, increasing load leads to increase in polymer viscosity, which can also cause CNTs aggregating in the matrix. Ashrafi investigated the SWCNT-modified epoxy sensor to monitor the crack evolution of the aluminium structure under fatigue loading. The mechanical test result demonstrated that CNT modification reduced the mechanical properties of the epoxy, which is caused by the poor decentralization of the CNT fillers. And the crack evolution process of the host aluminium structure could be inspected by monitoring the sensor current.¹⁰ Chou and colleagues^{11–13} investigated the delamination of CNT/fibre composite, where CNT distributed into composite matrix during its fabrication and formed the continuously conducting network in the matrix. The internal damage, such as delamination, matrix crack, will disrupt the conducting net and will cause the resistance of composite change. They successfully detected the composite joints' damage failure by this method. Buckypaper (BP) is a thin two-dimensional (2D) membrane with meso/macropore structure, which is only composed of random uniform distributed or aligned CNTs assembled by van der Waals forces among adjacent tubes.¹⁴ BP fabrication methods include filtration,¹⁵ chemical vapour deposition (CVD) growth¹⁶ and layer-by-layer deposition.¹⁷ Because BP is made up of CNTs, and the contract distance in the range of van der Waals force between connecting tubes, the contract resistance is relatively low. But BP also has piezo-resistive effect. Kang et al.¹⁸ and Wang et al.¹⁹ investigated the free-standing random distribution BP strain

sensing properties by cantilever beam bending and three-point bending experiment, respectively. The results demonstrated that the free-standing BP's in-plane tensile sensing properties are bad and emerge nonlinear. But Parmar et al.'s²⁰ work of the aligned BP revealed that the alignment BP had good in-plane sensing performance, especially in the direction perpendicular to the alignment.

From our former work,²¹ the BP is a 2D thin membrane with meso/macropore structure, and the epoxy resin has low contract angle (23°), which indicates that the epoxy resin can infiltrate inside the BP to form a BP/epoxy composite. The BP/epoxy composite possesses piezo-resistive effect and can act as strain sensor in CNT-modified epoxy composite. The BP/epoxy composite fabrication process can avoid the problems in CNT/epoxy composite, such as CNT aggregation, the resin viscosity increasing.

In summary, the uniformly distributed CNTs in the matrix can form continuous conducting network, which can be used to monitor the strain and detect damage of polymer and advanced fibre-reinforced polymer composite. Because of the large specific surface area of the CNTs, the dispersion of CNTs is key problem of CNTs filled composite, which affects its sensing and mechanical properties.

In this study, we propose a self-sensing fibre-reinforced polymer composite with embedded BP layer, where the BP just acts as strain and damage sensing layer based on piezo-resistive effect, but the fibre bears the loads. The BP sensing layer in the composite is a just a BP/polymer composite. We investigated the impact of BP sensing layer size on its sensing performance, by studying the different aspect ratios of BPs. And the strain and damage sensing performances of the self-sensing composite were investigated.

Experimental

Materials

In this study, the BP was made of highly purified SWCNT, which was purchased from Chengdu Organic Chemicals Co., Ltd, China. The outer diameter of the SWCNT is 1–2 nm, and the tube length ranges from 5 to 30 µm, which was synthesized by a chemical vapour deposition, whose purity is more than 95 wt%. Triton X100 (biochemical grade; Aladdin Chemical Reagents Co., Ltd, China) was used as a nonionic surfactant in BP fabrication progress. Bisphenol A type epoxy resin (EX-2511-1A; ShangWei Wind Power Material Co., Ltd, China) was used as composite matrix, the average viscosity of which ranges 900–1400 cps. An amine-type room temperature hardener (EX-2511-1BS; ShangWei Wind Power Material Co., Ltd) was employed. The

weight ratio of epoxy and hardener is 10:3, which cures at room temperature for 24 h.

BP, BP/epoxy composite and BP/glass fibre/epoxy composite preparation

BP fabrication. In this study, we employed the filtration process to fabricate the BP, which included CNT aqueous suspension preparation, vacuum filtration, water rinse and drying. A measure of 500 mg SWCNTs and 2.5 g Triton X100 and a volume of 5 L deionized (DI) water were mixed and stirred for 4 h, followed by four cycles of continuous ultrasonication (Vibra-Cell™, 700 W; Sonics, USA) with 50 mL/min liquid flow rate at 40% of the power. Then the dispersed CNTs suspension was vacuum filtrated with 0.45 mm porous diameter Nylon filtration membrane. The nanotubes uniformly deposited on the surface of the membrane. DI water was used to wash the CNT deposition on the membrane with the aid of vacuum, and then, it was dried in oven at 60 °C for 10 h. The free-standing BP peeled of the membrane after drying.

BP/epoxy film preparation. In this section, we wanted to investigate the impact of BP sensing dimension on the sensing properties of BP/epoxy composite; 10 mm width was employed and five aspect ratios of 3, 6, 9, 12 and 15 were used. Five BP/epoxy film samples were fabricated. We used two electrodes' method to measure the resistance of the BP sensing layer. The BP was cut into 10-mm-wide strips. Two copper wires (diameter: 0.1 mm) were bonded to the surface of the BP by conducting silver glue, and the spacing of the two electrodes is the length calculated by the aspect ratio. The BP

with electrodes was cured in oven at 120 °C for 2 h to make sure of the electrodes bonding to the BP. After the BPs (with electrodes) were infiltrated by epoxy resin (with hardener), it was compressed by two glass plates (which is disposed by release agent) to form a uniform thickness film and was cured for 24 h at room temperature. Because the composite was very thin and brittle, we prepared aluminium dog-bone-shaped plate as host structure. In the sensing test, the BP/epoxy film was bonding along the surface of the host plate.

BP/glass fibre/epoxy self-sensing composite preparation. In this section, we just investigated the strain sensing properties and damage detection of the glass fibre composite with embedded BP. The BP width was also 10 mm and the spacing 90 mm (aspect ratio = 9), in order to compare with the BP/epoxy film results. The whole dimension of the composite was $18 \times 200 \text{ mm}^2$ (width \times length). Four layers of orthogonal woven glass fibre fabric were used. The BP was placed on one surface of the composite, in the centre of the composite. The total thickness of the composite with embedded BP was 2 mm. Two samples were fabricated, one for cycle strain sensing test and the other for damage detection. To make sure the damage happened in the length range of BP, we made a V-notch at the centre of the BP length direction. The cone depth was 2.43 mm and the cone tip to BP edge was 1.6 mm. To compare with the BP detecting result, an electric strain gauge bonded along the edge of the BP and under the cone tip, as shown in Figure 1.

Characterization

The BP and its composite morphology were observed by Quanta 200 F field-emission scanning electron microscope (FE-SEM) with an operating voltage of 30 kV. Conductivity was measured using a Napson Resistivity Measurement System (RG-7C) Four-Point Probe with 0.4 mm probe tip diameter and 1.0 mm tip spacing.

As the piezo-resistive effect is the relation between deformation (or strain) and resistance change, the strain and damage sensing properties of the BP/epoxy films and BP/glass fibre/epoxy composites were determined on the static tension test frame (Shanghai Heng Wing Precision Instrument Co., Ltd; maximum tension force: 50 kN, China) for tensile deformation. The loading speed was controlled by the test frame beam displacement rate, which was 2.0 mm/min. The resistance change in BP in the two kinds of composites was measured by voltammetry method. And the measurement system composed of a constant current power supply (ITECH, USA) and a high-precision voltage

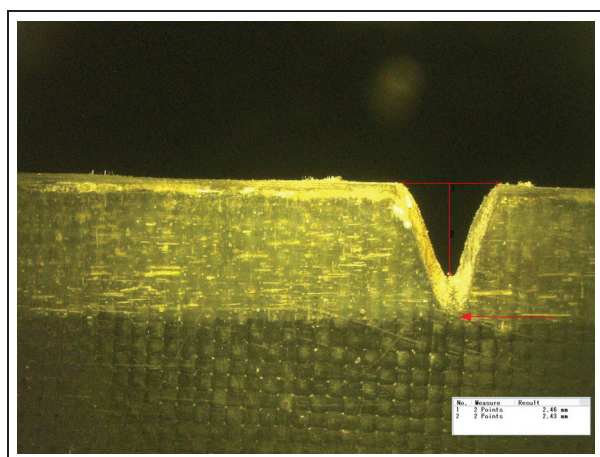


Figure 1. Self-sensing composite specimen for damage detecting with artificial V-notch damage (the horizontal red arrow indicates the edge of BP).

acquisition equipment (GL900-8; Graphtec, Japan), with electrical voltage recording resolution of 0.1 mV in 0–2 V measurement range and with the data sampling frequency of 100 Hz at most.

The resistance can be measured by the constant current supply power and high-resolution voltage acquisition instrument. The constant current power supply can supply constant current, and the current controlling resolution is 0.1 mA, the upper limits of current and voltage are 10 A and 100 V respectively; we used the voltage acquisition system to record the voltage implied on the testing BP composite samples and the system has eight channels; and in the range of 2 V, the voltage measurement resolution is 0.1 mV and the sample frequency can reach to 100 Hz. According to the current and voltage supply on the BP composite, according to Ohm's law, we can calculate the resistance. The strain of the composite was measured by electric strain gauge bonding on the surface of the sample, along the tensile direction. Three strain gauges were bonded along the length of the BP covering area, and the ultimate strain was the average of the three strains. The strain data sample frequency was 5 Hz.

Results and discussion

BP, BP/epoxy and self-sensing composite morphology

After fabrication, the free-standing BP with slide surface was formed. The BP has relatively high ductility, not as the normal paper's, but can satisfy composite

fabricating operation requirements, as shown in Figure 2(a). The morphology shown in Figure 2(b) and (c) indicated that the SWCNTs in BP appeared in rope form and the diameter is about 100 nm. And the SWCNT ropes lied randomly and flat to each other. And the pores in the BP were less than 100 nm in diameter, which existed in and between the SWCNT ropes as proven by our previous work.²¹

Figure 3(a) shows the SEM image of BP/epoxy film. The film is composed of BP and epoxy resin, and there are two epoxy-rich layers on both sides of the BP. Because there are pores inside the BP, epoxy resin can infiltrate into it. For the BP layer inside the BP/epoxy film, the epoxy resin fills the pore of the BP and forms a homogeneous structure. And there are no obvious bonding interfaces between the BP and epoxy, avoiding the delamination of the BP and epoxy matrix, which ensures the sensing BP deforming consistently with the composite film. The BP/glass fibre/epoxy self-sensing composite is a laminated structure, composed of the surface sensing BP/epoxy layer and main glass fibre-reinforced epoxy load-carrying layer, as demonstrated in Figure 3(b). Also because of the infiltration property of epoxy in the BP, there is a good bonding formed between the BP and the glass fibre/epoxy composite. And this can ensure that the deformation and penetrated crack of the load-carrying composite can transmit to the sensing BP/epoxy layer. From the above analysis, in the self-sensing composite, the bonding between the sensing element (BP layer) and measured

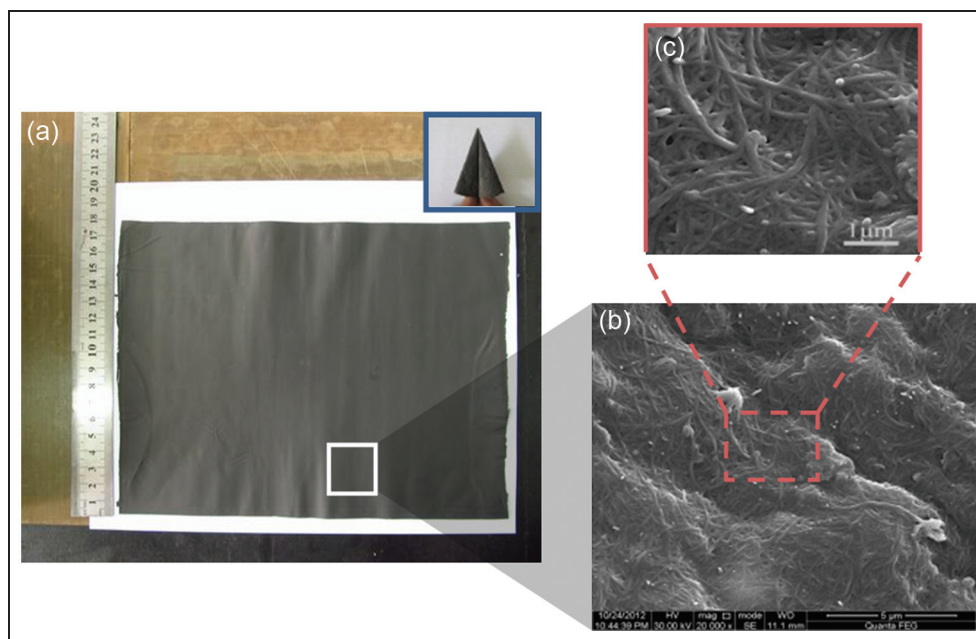


Figure 2. Photographs and FE-SEM images of the free-standing buckypaper and its morphology. (a) the photo of BP and paperfolding plane made of BP, (b) FE-SEM image of BP, (c) the enlarged view of (b).

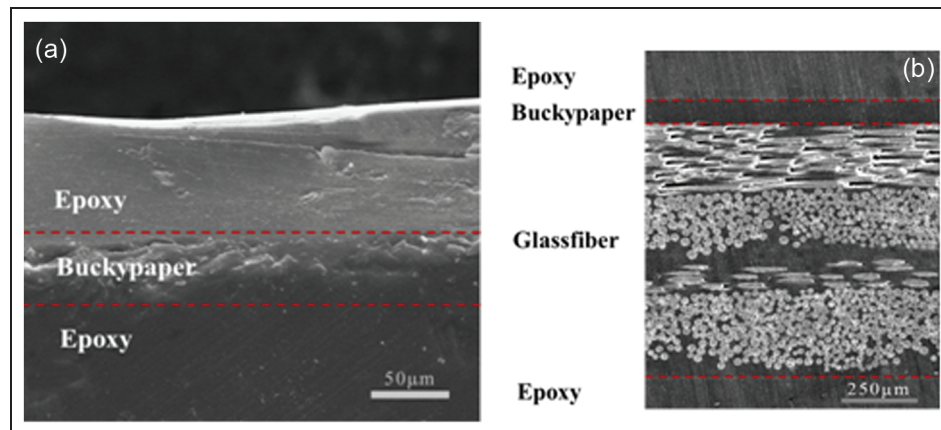


Figure 3. FE-SEM images of BP/epoxy film and BP/glass fibre/epoxy self-sensing composite: (a) BP/epoxy film and (b) BP/glass fibre/epoxy self-sensing composite.

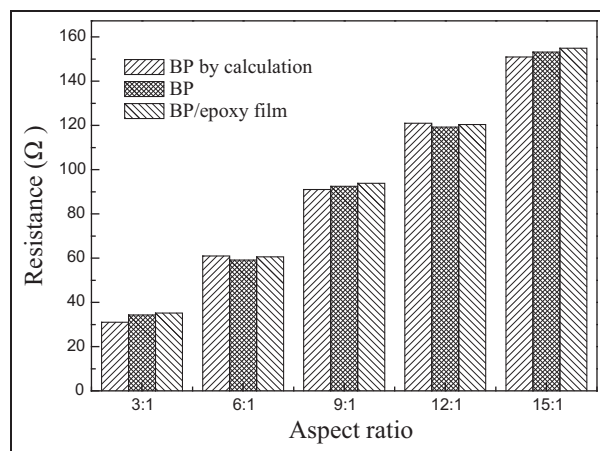


Figure 4. Resistance between electrodes of BP and BP/epoxy film for different aspect ratios.

object (the glass fibre-reinforced composite) is guaranteed for strain and damage monitoring.

BP, BP/epoxy and self-sensing composite electrical properties

The resistivity of the BP (thickness: 50 μm) was measured by four-point probe method. The average resistivity was 0.05 Ωcm . The resistivity of single SWCNT is less than $10^{-4}\Omega\text{cm}$, depending on its chiral structure. But why the BP show high resistivity comparing to single SWCNT? The BP is made of CNTs by the van der Waals forces between CNTs, and there exist contact resistance between CNTs, which cause the relatively high resistivity than single CNT. And the contact resistance is dominated by the contact distance between the two tubes according to the tunnelling effect. To discuss the epoxy infiltration effect on the resistivity of BP, we investigated

the resistances of BP (thickness: 50 μm , width: 10 mm, resistivity: 0.05 Ωcm , with a pair of wire electrode resistance: 0.9 Ω) and after epoxy infiltration (in the BP/epoxy film) with five different aspect ratios (different electrode distances). The results are illustrated in Figure 4, where the bars of BP by calculation were calculated according to the law of resistance. Figure 4 demonstrates that the calculation, before and after infiltration resistances corresponding to the aspect ratio, has the same tendency, but with little difference, which proves that resistance of BP before and after epoxy infiltration approximately obeys the law of resistance. But there are no consistent results with different aspect ratios. It is because the calculating results just consider the resistance of the BP (composing resistances of CNTs and contact resistances) and electrode wire resistance, but experimental BP's resistance result is composed of the resistance of BP, resistance of the electrode wire the same as calculation and also resistance change caused by bonding electrode, which lead to the change in aspect ratio or introduced additional contact resistance between electrodes and BP. To the BP and the BP/epoxy film, the resistances increased with increasing of the aspect ratio, but to the same aspect ratio, the resistance of BP/epoxy film is larger than the BP's. The resistances of the BP and BP/epoxy film of the each aspect ratio are measured on the same BP with affirmative electrodes. The resistance change is caused by two contrary reasons, one is epoxy infiltrates between CNTs, which increases the resistance; the other is decrease in distances between connecting CNTs caused by the chemical shrinkage during epoxy consolidation, which lead to the decrease in resistance.

Self-strain sensing properties of BP/epoxy film

Because in self-sensing composite embedded with BP layer the sensing layer is just as the form of BP/epoxy

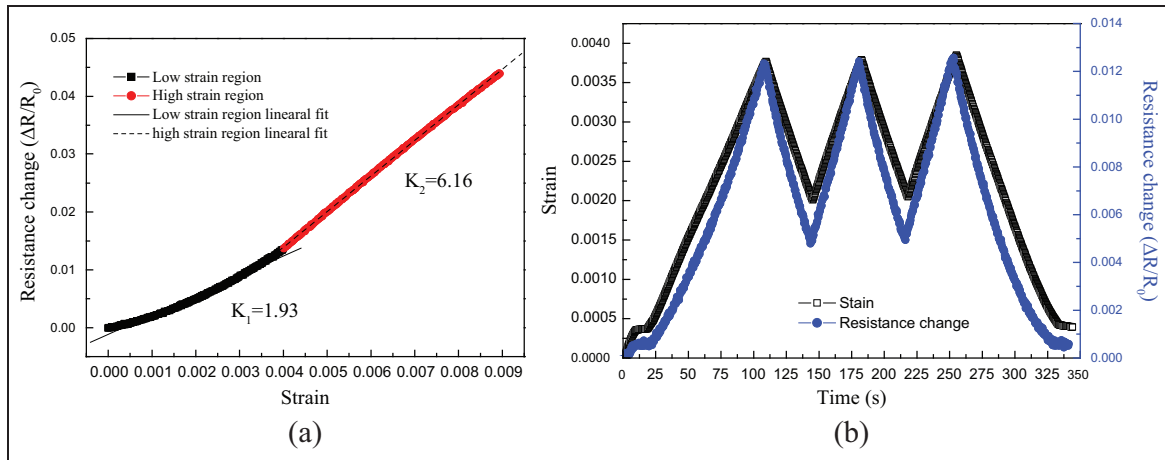


Figure 5. Sensing properties of BP/epoxy film with buckypaper aspect ratio of 3:1: (a) relation between strain and resistance change and (b) cycling correlation between strain, resistance change and time.

film, we investigated the effect of the BP sensing layer dimension on the strain sensing properties by BP/epoxy film low strain level cycling tension and high strain level tension experiments. Figures 5 to 10 show the tensile and cycling sensing performance of the BP/epoxy film with different aspect ratios. From part (a) of Figures 5 to 9, the resistance change in the film and strain were nonlinearly related for whole tensile process. But it can be divided into stages such as low-strain nonlinear stage and high-strain linear stage.

The strain sensing of the BP/epoxy film was dependent on the piezo-resistivity, but it is different from the free-standing BP. To free-standing BP, because the poor bonding between CNTs, which is mainly produced by van der Waals force and the tubes entanglement, the piezo-resistivity is dominated by tubes contact distance and area, almost no intrinsic resistance change happen to the CNTs. But to the BP inside the epoxy, because of the resin bonding effect, the CNTs can consistently deform with the matrix, which cause the CNTs' intrinsic resistance change obviously. And at the same time, the restriction of the matrix limits the contact resistance change. The piezo-resistivity effect of BP/epoxy film is dominated by the resistance change in CNTs, so BP/epoxy film shows better strain sensing abilities compared to free-standing BP.

During the infiltration epoxy resin consolidation process among the random distributing CNTs in BP, non-uniformly distributed residual stress (strain) will exist in the CNTs. Under low strain level, the residual stress or strain of the CNTs in BP redistribute, and the resistance change is nonlinear to out strain; after residual strain distribution, with the increasing of out strain, the CNTs deform in accordance with out deformation, and resistance change will be linearly related to out strain.

To characterize strain sensing property of the BP/epoxy film, the gauge factor was introduced

$$K = \frac{\Delta R/R_0}{\varepsilon} \quad (1)$$

where R_0 is the resistance of the BP/epoxy film without strain and ΔR is the BP/epoxy film resistance change under certain strain (ε). To simplify the tensile process, we regarded the low and high strain levels as two regions of part (a) of Figures 5 to 9, respectively, and linear fittings were performed to each regions. And the gauge factors of the low and high strain levels in each aspect ratio BP/epoxy film were obtained, as shown in Figure 10(b). The gauge factors in high strain level were almost the same (about 6.20) for the five different aspect ratios of BP/epoxy film. But to the low strain region, the gauge factors were different from different aspect ratio BP/epoxy films. That's because that, to the low strain region, the resistance change is nonlinear to strain. In this paper the gauge factor of this region was got by linear fitting, and existed large errors. Figure 10(a) shows the resistance change versus strain curve of five different aspect ratios of BP/epoxy films; the absolute resistance change in the BP film with 3:1 aspect ratio is lower than other aspect ratios, which is caused by relatively lower zero strain resistance of the BP, but have no influence on the gauge factor at the high-strain region. The cycling tension testing results shown in part (b) of Figures 5 to 9 indicated that the resistance change developed consistently with strain; there was no hysteresis for the resistance change.

Strain and damage sensing of the self-sensing composite with embedded BP layer

From the above BP/epoxy film tensile strain sensing and cycling results, we investigated the strain sensing

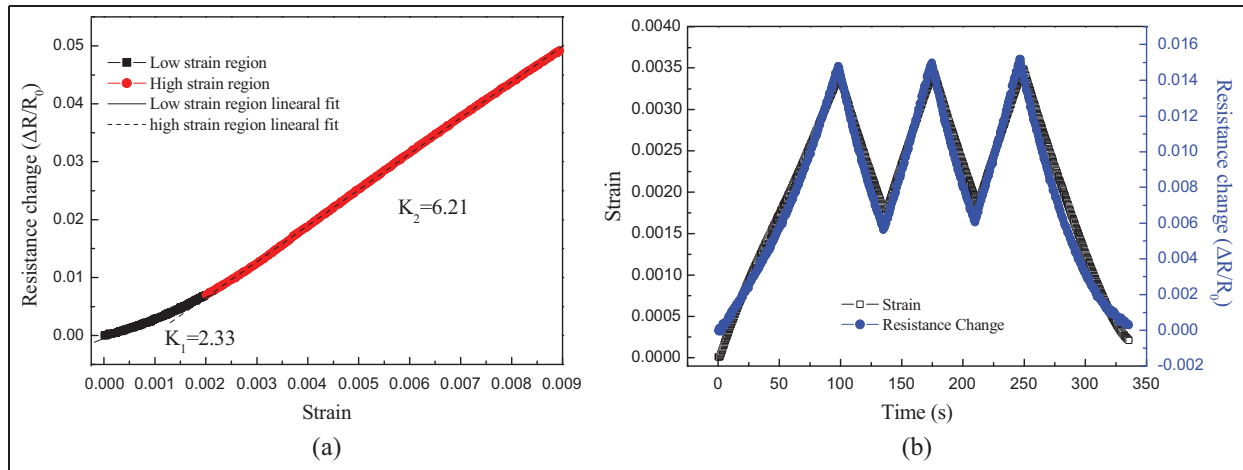


Figure 6. Sensing properties of BP/epoxy film with buckypaper aspect ratio of 6:1: (a) relation between strain and resistance change and (b) cycling correlation between strain, resistance change and time.

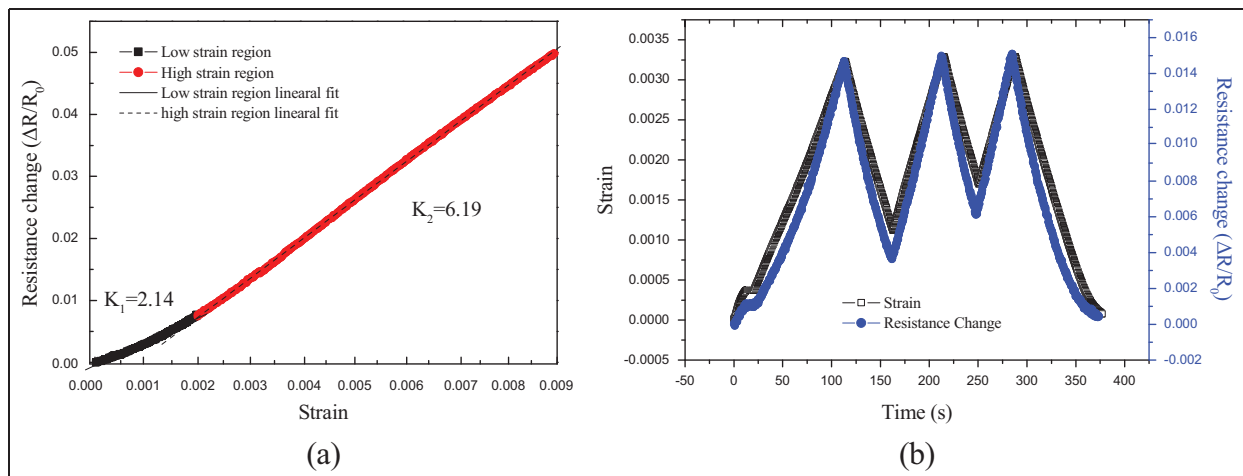


Figure 7. Sensing properties of BP/epoxy film with buckypaper aspect ratio of 9:1: (a) relation between strain and resistance change of film and (b) cycling correlation between strain, resistance change and time.

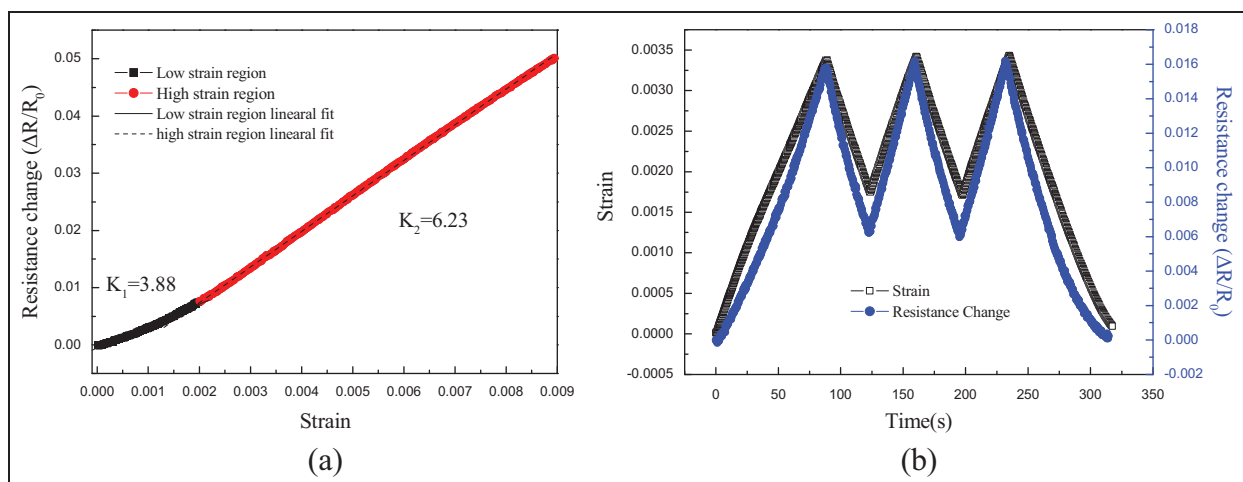


Figure 8. Sensing properties of BP/epoxy film with buckypaper aspect ratio of 12:1: (a) relation between strain and resistance change and (b) cycling correlation between strain, resistance change and time.

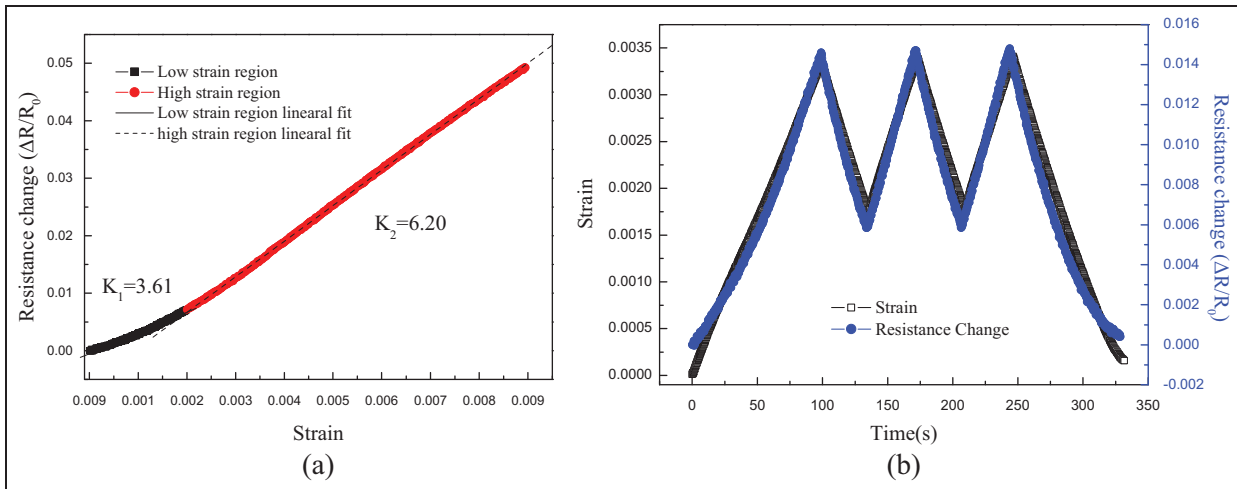


Figure 9. Sensing properties of BP/epoxy film with buckypaper aspect ratio of 15:1: (a) relation between strain and resistance change and (b) cycling correlation between strain, resistance change and time.

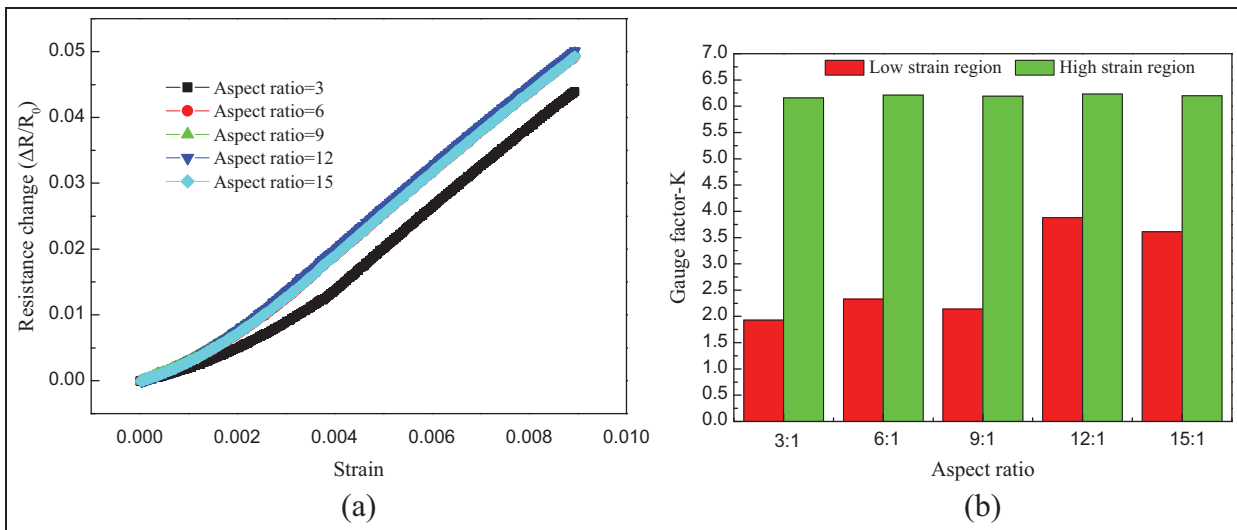


Figure 10. The BP/epoxy film sensing properties with five aspect ratios: (a) relation between strain and resistance change and (b) gauge factors.

and damage detecting properties of glass fibre/epoxy composite embedded with BP layer (width: 10 mm, aspect ratio: 9:1).

The strain sensing results shown in Figure 11 exhibited that the self-sensing composite had the same gauge factor and cycling performance as BP/epoxy film under high strain level and bad strain sensing performance under low strain level, which indicated that the strain sensing properties of the BP composite were unaffected by the fabrication process. In order to study the damage detection ability of the composite using embedded BP layer, we explored the resistance revolution process of the same self-sensing composite as above with an

artificial side penetrating V-notch damage under tension till breaking, as shown in Figure 12. Before the strain of composite at the edge of BP beside the notch tip arrived at about 0.1%, the strain and resistance change increased linearly with time. There was a fibre cracking sound as the composite strain reaching to 0.1%, accompanied with the sharp increase of the strain monitored by the electrical strain gauge bonding beside the notch. At the same time, the resistance of the BP increased substantially. Within no more than 20 s, the composite sample broke completely at the notch and the resistance of the BP inside the composite became infinity. In the testing process, before the sound

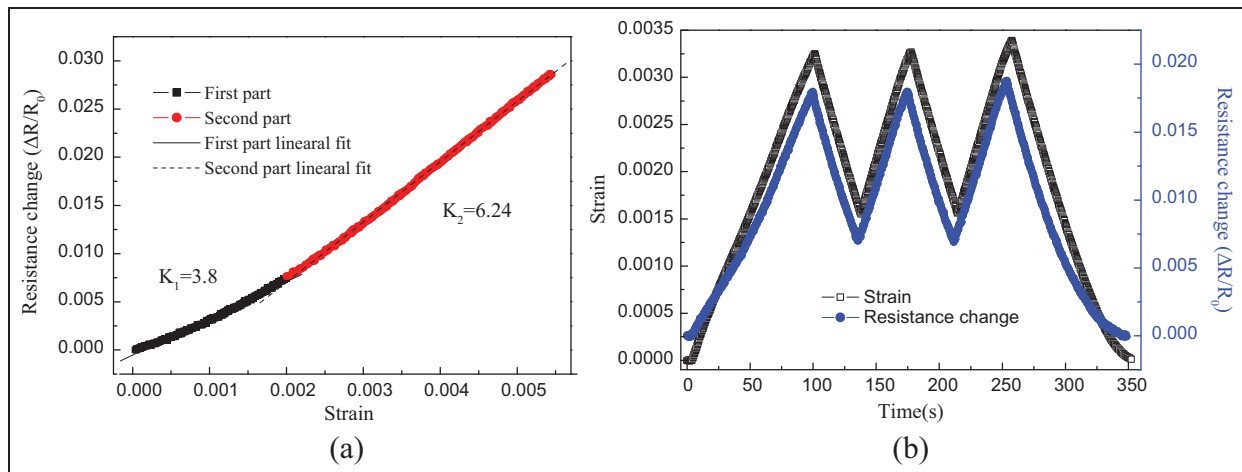


Figure 11. Sensing properties of BP/glass fibre/epoxy self-sensing composite with buckypaper aspect ratio of 9:1: (a) relation between strain and resistance change and (b) cycling correlation between strain, resistance change and time.

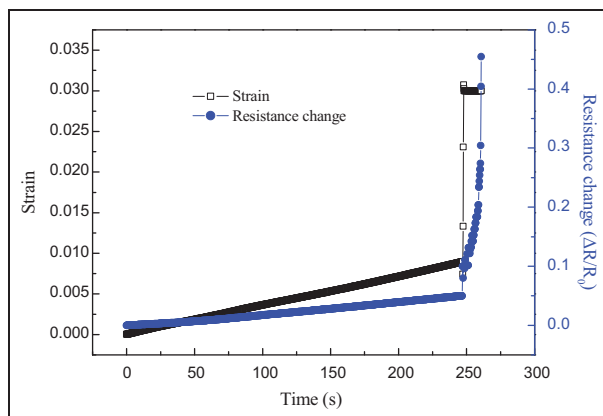


Figure 12. Correlation between strain and resistance change during tensile failure process of BP/glass fibre/epoxy self-sensing composite with artificial V-notch damage.

of fibre cracking, there were no damages (fibre breaking, delamination and matrix cracking) happening to the composite, only concentrating strain exerting on the strain gauge and BP. But after the fibre breaking, the crack in the composite at the notch expanded to the strain gauge leading to sharp increase in strain measured by strain gauge; at the same time, the crack penetrated into the BP and decreased the effective width of the sensing BP layer, causing the resistance change increasing obviously. When the crack of the composite reached to some extent, the de-bonding will happen between the strain gauge and the composite. But because the width of BP was wider than strain gauge, and embedded in the composite, the BP sensing layer can record the crack evolution process until totally breaking.

Conclusion

This study proposed a self-sensing fibre-reinforced composite, which could monitor the strain and detect damage of the composite by embedded BP sensing layer based on its piezo-resistivity effect. The relations between resistance change and strain of BP/epoxy film, as the sensing layer in the self-sensing composite, indicated that the BP film had high sensitivity at high strain level (above $2000 \mu\epsilon$), with gauge factor about 6.2, and had good cycling repeatability. And the above sensing properties were independent of the size of BP sensing layer, which could be used in long and small gauge length according to monitoring requirements. The strain and damage sensing of self-sensing fibre-reinforced composite shows that the composite did not only show high sensitivity of strain but also records the damage development of the composite. The embedded BP sensing layer is a promising approach for fibre-reinforced composite structural health monitoring.

Declaration of conflicting interests

The authors declare that there is no conflict of interest.

Funding

This article was supported by NSF (grant No. 51108131) and, in part, by the Fundamental Research Funds for the Central University (Grant No. HIT NSRIF 2014030).

References

1. Zhao XF, Gou JH, Song GB, et al. Strain monitoring in glass fiber reinforced composites embedded with carbon

- nanopaper sheet using Fiber Bragg Grating (FBG) sensors. *Compos Part B: Eng* 2009; 40: 134–140.
2. Fernando GF, Hameed A, Winter D, et al. Structural integrity monitoring of concrete structures via optical fiber sensors: sensor protection systems. *Struct Health Monit* 2003; 2(2): 123–135.
3. Leng JS and Asundi A. Real-time cure monitoring of smart composite materials using extrinsic Fabry-Perot interferometer and fiber Bragg grating sensors. *Smar Mat St* 2002; 11: 249–255.
4. Su ZQ, Ye L and Lu Y. Guided Lamb waves for identification of damage in composite structures: a review. *J Sound Vib* 2006; 295: 753–780.
5. Gou JH, Minaie B, Wang B, et al. Computational and experimental study of interfacial bonding of single-walled nanotube reinforced composites. *Comp Mater Sci* 2004; 31(3–4): 225–236.
6. Lau KT, Shi SQ, Zhou L-M, et al. Micro-hardness and flexural properties of randomly-oriented carbon nanotube composites. *J Compos Mater* 2003; 37(4): 365–376.
7. Bautista-Quijano JR, Aviles F, Aguilar JO, et al. Strain sensing capabilities of a piezoresistive MWCNT-polysulfone film. *Sensor Actuat A: Phys* 2010; 159(2): 135–140.
8. Baltopoulos A, Athanasopoulos N, Fotiou I, et al. Sensing strain and damage in polyurethane-MWCNT nanocomposite foams using electrical measurements. *Express Polym Lett* 2013; 7(1): 40–54.
9. Bilotti E, Zhang R, Deng H, et al. Fabrication and property prediction of conductive and strain sensing TPU/CNT nanocomposite fibres. *J Mater Chem* 2010; 20(42): 9449–9455.
10. Ashrafi B, Johnson L, Martinez-Rubi Y, et al. Single-walled carbon nanotube-modified epoxy thin films for continuous crack monitoring of metallic structures. *Struct Health Monit* 2012; 11(5): 589–601.
11. Thostenson ET and Chou TW. Carbon nanotube-based health monitoring of mechanically fastened composite joints. *Compos Sci Technol* 2008; 68: 2557–2561.
12. Thostenson ET, Chou TW. Carbon Nanotube networks: sensing of distributed strain and damage for life prediction and self Healing. *Adv Mater* 2006; 18: 2837–2841.
13. Li CY, Thostenson ET and Chou TW. Sensors and actuators based on carbon nanotubes and their composites: a review. *Compos Sci Technol* 2008; 68(6): 1227–1249.
14. Smajda R, Konya Z and Kiricsi I. Controlling the pore diameter distribution of multi-wall carbon nanotube buckypapers. *Carbon* 2007; 45: 1696–1698.
15. Wu Z, Chen Z, Du X, et al. Transparent, conductive carbon nanotube films. *Science* 2004; 305(5688): 1273–1276.
16. Ma W, Song L, Yang R, et al. Directly synthesized strong, highly conducting, transparent single-walled carbon nanotube films. *Nano Lett* 2007; 7(8): 2307–2311.
17. Srivastava S, Podsiadlo P, Critchley K, et al. Single-walled carbon nanotubes spontaneous loading into exponentially grown LBL films. *Chem Mater* 2009; 21(19): 4397–4400.
18. Kang I, Schulz M, Kim JH, et al. A carbon nanotube strain sensor for structural health monitoring. *Smar Mat St* 2006; 15: 737–748.
19. Wang YT, Liu ZD, Yi J, et al. Study on the piezoresistive effect of the multiwalled carbon nanotube films. *Acta Phys Sin* 2012; 61(5): 057302.
20. Parmar K, Mahmoodi M, Park C, et al. Effect of CNT alignment on the strain sensing capability of carbon nanotube composites. *Smar Mat St* 2013; 22(7): 075006.
21. Chu HT, Zhang ZC, Liu YJ, et al. Self-heating fiber reinforced polymer composite using meso/macropore carbon nanotube paper and its application in deicing. *Carbon* 2014; 66: 154–163.